Cell Reports
Article

Cell PRESS
Open ACCESS

TERRA-Reinforced Association of LSD1 with MRE11 Promotes Processing of Uncapped Telomeres

Antonio Porro,[1,2,3] Sascha Feuerhahn,[1,2] and Joachim Lingner[1,*]
[1]ISREC-Swiss Institute for Experimental Cancer Research, School of Life Sciences, EPFL-Ecole Polytechnique Fédérale de Lausanne, Lausanne 1015, Switzerland
[2]These authors contributed equally to this work
[3]Present address: Institute of Molecular Cancer Research, University of Zürich, Zürich 8057, Switzerland
*Correspondence: joachim.lingner@epfl.ch
http://dx.doi.org/10.1016/j.celrep.2014.01.022

SUMMARY

Telomeres protect chromosome ends from being recognized as sites of DNA damage. Upon telomere shortening or telomere uncapping induced by loss of telomeric repeat-binding factor 2 (TRF2), telomeres elicit a DNA-damage response leading to cellular senescence. Here, we show that following TRF2 depletion, the levels of the long noncoding RNA TERRA increase and LSD1, which binds TERRA, is recruited to telomeres. At uncapped telomeres, LSD1 associates with MRE11, one of the nucleases implicated in the processing of 3′ telomeric G overhangs, and we show that LSD1 is required for efficient removal of these structures. The LSD1-MRE11 interaction is reinforced in vivo following TERRA upregulation in TRF2-deficient cells and in vitro by TERRA-mimicking RNA oligonucleotides. Furthermore, LSD1 enhances the nuclease activity of MRE11 in vitro. Our data indicate that recruitment of LSD1 to deprotected telomeres requires MRE11 and is promoted by TERRA. LSD1 stimulates MRE11 catalytic activity and nucleolytic processing of uncapped telomeres.

INTRODUCTION

Telomeres are the nucleoprotein caps that protect the ends of linear chromosomes from being recognized as sites of DNA damage (de Lange, 2009). Due to the end-replication problem and nucleolytic processing, gradual attrition of telomere length occurs with aging (Baird, 2008). The proper maintenance of telomeres is crucial for chromosome stability. Loss or damage of the chromosome ends initiates a DNA-damage response (DDR) and triggers replicative senescence (d'Adda di Fagagna et al., 2003; Deng et al., 2008; Denchi and de Lange, 2007; Takai et al., 2003).

Mammalian telomeres consist of double-stranded 5′-TTAGGG-3′/5′-CCCTAA-3′ repeats terminating in 3′ protruding single-stranded G-rich overhangs. Telomeric DNA is associated with specialized telomeric proteins that are known as shelterins (de Lange, 2005). Shelterins play crucial roles in protecting chromosome ends from DNA-damage checkpoint signaling and DNA repair (de Lange, 2009). Telomeric repeat-binding factors 1 and 2 (TRF1 and TRF2) bind directly the double-stranded telomeric DNA recruiting TIN2, TPP1, and Rap1 to telomeres (de Lange, 2005). POT1 in association with its binding partner TPP1 binds the single-stranded 3′ G-rich overhangs (Baumann and Cech, 2001). TRF2-depleted telomeres as well as critically short telomeres elicit a robust ATM-mediated DDR (Denchi and de Lange, 2007; Karlseder et al., 1999; Okamoto et al., 2013), which involves formation of "telomere dysfunction-induced foci" (TIFs) (Takai et al., 2003). TRF2-depleted telomeres undergo telomere fusion events by nonhomologous end-joining (NHEJ) (Celli and de Lange, 2005). It has been proposed that TRF2-mediated capping involves formation of t loop structures in which the telomeric 3′ G overhang is tucked into the double-stranded part of the telomeric DNA (Griffith et al., 1999). Consistent with this notion, t loop formation depends on TRF2 (Doksani et al., 2013).

Telomere end fusions upon TRF2 removal are induced by NHEJ and require prior removal of the telomeric 3′ G overhangs (Celli and de Lange, 2005; van Steensel et al., 1998). G overhang removal involves at least two protein complexes with nuclease activity: XPF/ERCC1 and MRE11/RAD50/NBS1. XPF-deficient human cells have diminished G strand overhang loss upon expression of the dominant-negative $TRF2^{\Delta B\Delta M}$ allele, and $Ercc1^{-/-}$ mouse embryonic fibroblasts (MEFs) are protected from telomere end fusions upon expression of $Trf2^{\Delta B\Delta M}$ (Zhu et al., 2003). Cells from the hypomorphic mouse mutant $Mre11^{ATLD1/ATLD1}$, which have defects in the ATM-dependent DDR, retain G strand overhangs upon deletion of *Trf2* and have reduced chromosome end fusions (Attwooll et al., 2009). This effect can be explained by the necessity of checkpoint activation to promote NHEJ at uncapped telomeres (Denchi and de Lange, 2007). However, in the presence of the presumed nuclease-deficient $Mre11^{H129N}$ allele, which is proficient in checkpoint signaling, 3′ G strand overhangs were also retained in *Trf2*-deleted cells. This therefore indicates that in addition to its roles in ATM activation, the nuclease activity of MRE11 is required for telomere 3′ end processing (Deng et al., 2009a).

Although tightly packaged as heterochromatin, telomeres are transcribed into a long noncoding RNA containing UUAGGG

repeats, referred to as TERRA. TERRA is an RNA polymerase II (RNAPII) transcript conserved throughout eukaryotes. It is transcribed from subtelomeres toward chromosome ends (Azzalin et al., 2007; Schoeftner and Blasco, 2008). TERRA remains partly associated with telomeric chromatin and is regulated in a cell-cycle-dependent manner, with low levels occurring in late S phase (Azzalin et al., 2007; Deng et al., 2009b; Feuerhahn et al., 2010; Porro et al., 2010). The nonsense-mediated mRNA decay (NMD) factors regulate TERRA presence at telomeres (Azzalin et al., 2007). TERRA transcription has been linked to chromatin structure. TERRA expression is repressed by the DNA methyltransferase enzymes DNMT1 and DNMT3b, which methylate CpG dinucleotides present in the human subtelomeric region (Nergadze et al., 2009; Yehezkel et al., 2008). Moreover, also the SUV39H1 H3K9 histone methyltransferase and heterochromatin protein 1α (HP1α), which binds H3K9me3, negatively regulate TERRA transcription (Arnoult et al., 2012). TERRA has been implicated in telomere length control. TERRA binds and represses telomerase (Redon et al., 2010; Schoeftner and Blasco, 2008), but this effect can be alleviated by TERRA binding proteins (Redon et al., 2013). Induction of TERRA in *Saccharomyces cerevisiae* leads to telomere shortening in *cis* through stimulation of exonuclease I (Exol) rather than through inhibition of telomerase (Pfeiffer and Lingner, 2012). Furthermore, TERRA foci in *S. cerevisiae* can trigger the assembly of telomerase into large clusters prior to their recruitment to short telomeres (Cusanelli et al., 2013). TERRA has also been proposed to regulate the exchange of RPA by POT1 at single-stranded telomeric DNA at the end of S phase (Flynn et al., 2011).

Lysine-specific demethylase 1 (LSD1) (also known as KDM1 and AOF2) is an amine oxidase that catalyzes lysine demethylation in a flavin adenine dinucleotide (FAD)-dependent oxidative reaction (Lan et al., 2008; Shi et al., 2004). LSD1 removes mono- and dimethyl groups from lysine 4 (H3K4) (Shi et al., 2004) and lysine 9 (H3K9) (Metzger et al., 2005) of histone 3. LSD1 also acts on nonhistone proteins including p53, E2F1, and DNMT1 (Huang et al., 2007; Kontaki and Talianidis, 2010; Wang et al., 2009).

Here, we discover that TERRA collaborates with LSD1 and MRE11 at uncapped telomeres. Upon TRF2 depletion, TERRA expression increases, and LSD1 is tethered to telomeres. LSD1 recruitment to dysfunctional telomeres requires the MRN complex and is stimulated by TERRA, which associates with LSD1 and enhances the binding affinity between LSD1 and MRE11. LSD1 has no visible impact on the chromatin state of uncapped telomeres, but it is required for the nucleolytic removal of the telomeric 3′ G overhang. Because LSD1 stimulates MRE11 nuclease activity in vitro, it may promote removal of 3′ G overhangs at dysfunctional telomeres through MRE11 in vivo. Our data indicate that TERRA and LSD1 cooperate to regulate MRE11 activity for the processing of uncapped telomeres.

RESULTS

Telomere Deprotection Modulates TERRA Association with LSD1

Telomere uncapping induced by TRF2 knockdown leads to TERRA upregulation in human fibroblasts (Caslini et al., 2009). We observed that also in HeLa cells, functional small hairpin RNA (shRNA)-mediated depletion of TRF2 (Figures S1A and S1B) leads to TERRA accumulation (Figure 1A, lower panel). Because TERRA may participate in telomeric heterochromatin formation (Arnoult et al., 2012; Deng et al., 2009b), we hypothesized that it might assemble chromatin-modifying complexes at dysfunctional telomeres in analogy to other long noncoding RNAs like Xist and HOTAIR, which also regulate chromatin (Penny et al., 1996; Tsai et al., 2010; Wutz et al., 2002). In order to identify chromatin-remodeling complexes that are associated with TERRA, we performed native RNA immunoprecipitation experiments with several RNA binding proteins and chromatin-modifying enzymes (data not shown). Immunoprecipitation of endogenous LSD1 from HEK293T and HeLa cells specifically retrieved endogenous TERRA, but not U2 small nuclear RNA (snRNA) or 18S rRNA (Figures S1C and S1D, lower panels). Because a substantial fraction of TERRA interacts with hnRNP A1 (Redon et al., 2013), immunoprecipitation of endogenous hnRNP A1 was used as positive control (Figure S1C, lower panel). To rule out potential nonspecific interactions and to determine whether the association between TERRA and LSD1 was not occurring postlysis in nuclear extracts, we further performed analogous RNA immunoprecipitation experiments with formaldehyde-crosslinked HeLa cells followed by stringent washing conditions. Consistent with a bona fide interaction, we observed that 2%–3% of TERRA was immunoprecipitated with antibodies against endogenous LSD1, whereas TERRA did not immunoprecipitate with IgG control (Figure 1A, lower panel). Several cytoplasmic, mitochondrial, and nuclear RNAs were not associated with LSD1 as assessed by RNA immunoprecipitation of crosslinked extracts (Figure S1E, lower panel), whereas HOTAIR, which was previously shown to be associated with LSD1-containing complexes (Tsai et al., 2010), served as a positive control (Figure S1E, lower panel). Although the fraction of TERRA bound by LSD1 was similar in wild-type (WT) cells (shEV) and cells depleted for TRF2 (shTRF2), the absolute amounts of TERRA-LSD1 complexes increased upon TRF2 removal, presumably due to the higher levels of TERRA that became available for binding to LSD1 (Figure 1A, lower panel). To further confirm the specificity of the association between LSD1 and TERRA, we ectopically expressed HA-tagged LSD1 from transiently transfected plasmids in HEK293T cells (Figure 1B). Approximately 2% of TERRA was specifically immunopurified with HA-tagged LSD1, whereas no TERRA was detected in extracts derived from empty vector control cells incubated with HA antibody (Figure 1B, lower panel). For all these experiments, the levels of recovered proteins with respect to the input confirmed an efficient immunoprecipitation (Figures 1A, 1B, and S1C–S1E, upper panels). Notably, the percentage of TERRA that associates with LSD1 is comparable to the fraction of TERRA bound to TRF1 and TRF2 (Deng et al., 2009b). Together, these experiments indicate that TERRA is associated with LSD1 in vivo.

LSD1 Binds the UUAGGG Repeat Array of TERRA Transcripts through Its SWIRM/AOL-N-ter Domain

To determine whether LSD1 interacts with TERRA directly and to assess sequence requirements, we carried out RNA

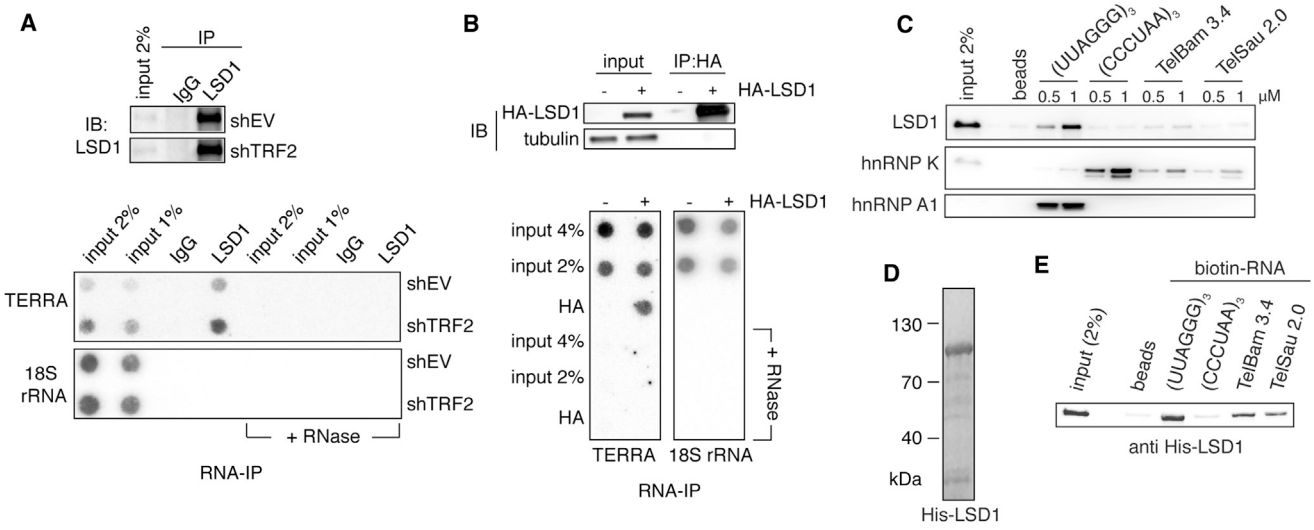

Figure 1. LSD1 Binds TERRA In Vivo and In Vitro

(A) Western blotting was used to evaluate immunoprecipitation (IP) efficiency of endogenous LSD1 in RNA-IP experiments (upper panel). RNA-IP assays with an antibody against endogenous LSD1 were performed in HeLa cells transfected with control vector (shEV) or depleted for TRF2 (shTRF2). IP-recovered RNA was detected with probes annealing with TERRA or 18S rRNA (lower panel). IB, immunoblot.

(B) Western blotting was used to evaluate immunoprecipitation efficiency of ectopic HA-LSD1 in RNA-IP experiments (upper panel). RNA-IP assays with HA antibody were performed in HEK293T cells transfected with HA-tagged LSD1 or expression vector alone. IP-recovered RNA was detected with probes annealing with TERRA or 18S rRNA (lower panel).

(C) Western blotting was used to detect the binding of LSD1, hnRNP A1, and hnRNP K in HeLa nuclear extracts to NeutrAvidin bead-bound biotinylated $(UUAGGG)_3$, $(CCCUAA)_3$, TelBam3.4, or TelSau2.0 RNA oligonucleotides.

(D) Coomassie staining was used to detect His-LSD1 affinity purified from *E. coli*.

(E) Western blotting was used to evaluate the capturing of bacterial-expressed and Ni-NTA-purified His-LSD1 on bead-coupled $(UUAGGG)_3$, $(CCCUAA)_3$, or subtelomeric sequences containing TelBam3.4 and TelSau2.0 RNA oligonucleotides.

EV, empty vector; HA, hemagglutinin; His, histidine. See also Figure S1.

pull-down experiments. TERRA molecules consist of subtelomeric- and telomeric-derived sequences. Immobilized biotinylated $(UUAGGG)_3$ RNA oligonucleotide (TERRA), but not antisense $(CCCUAA)_3$ (ARRET) or subtelomeric sequences containing RNA oligonucleotides (TelBam3.4 and TelSau2.0), retained LSD1 from HeLa nuclear extracts (Figure 1C) and purified His-LSD1 (Figures 1D and 1E). HnRNP K and hnRNP A1, which bind to C-rich and G-rich RNAs (Burd and Dreyfuss, 1994; Klimek-Tomczak et al., 2004; Thisted et al., 2001), respectively, were detected as controls (Figure 1C).

We next delineated the TERRA interaction domains of LSD1. Glutathione S-transferase (GST)-LSD1 fragments were expressed in *E. coli*, purified and incubated with bead-coupled TERRA-mimicking oligonucleotides $(UUAGGG)_3$ (Figures 2A–2C). Full-length (FL) LSD1 and LSD1 fragments encompassing the SWIRM and parts of the AOL domain (SWIRM/AOL-N-ter) were retained on the beads specifically in the presence of TERRA-mimicking $(UUAGGG)_3$ oligonucleotides (Figure 2C). The biochemical properties of the recombinant GST-SWIRM/AOL-N-ter domain of LSD1 were further characterized in electrophoretic mobility shift assays (EMSAs). The binding affinity of purified LSD1 (Figure S2A) for RNA increased with oligonucleotide length (Figure S2B). The dissociation constant of the RNA binding domain of LSD1 for $(UUAGGG)_{10}$ was 70 ± 1 nM (Figures 2D and 2E), whereas DNA of the same sequence was not bound (Figure S2C). FL HA-tagged LSD1 had similar binding affinity for $(UUAGGG)_{10}$ as GST-LSD1 (1–382) (data not shown). Binding specificity was further addressed by EMSA in competition experiments in which the binding to labeled $(UUAGGG)_{10/7}$ TERRA repeats was challenged with excess of unlabeled subtelomeric (Figure 2F) oligonucleotides or WT and mutant telomeric repeats (Figure 2G). RNA oligonucleotides mimicking subtelomeric elements barely competed (Figure 2F), and LSD1 showed specificity for the AGGG sequence within the UUAGGG repeats, but it did not recognize the UU dinucleotide (Figure 2G). We conclude that LSD1 associates directly via its SWIRM/AOL-N-ter domain with TERRA, with moderate sequence specificity for the WT UUAGGG repeat array of the transcript.

LSD1 Binding to Telomeres Is Increased upon TRF2 Depletion and Correlates with TERRA Levels

Because LSD1 associates with TERRA and because TERRA is a component of telomeric chromatin (Azzalin et al., 2007), we reasoned that LSD1 might also be physically bound to telomeres. To test this, we performed chromatin immunoprecipitation (ChIP) experiments with an antibody against endogenous LSD1 followed by dot blot analysis. We found telomeric DNA but not centromeric DNA in association with LSD1 (Figures 3A and 3B). The telomeric signal diminished upon shRNA-mediated depletion of LSD1, confirming the specificity of the antibody (Figures 3A and 3B). Interestingly, the telomeric signal in the LSD1-ChIP significantly increased upon telomere uncapping by TRF2

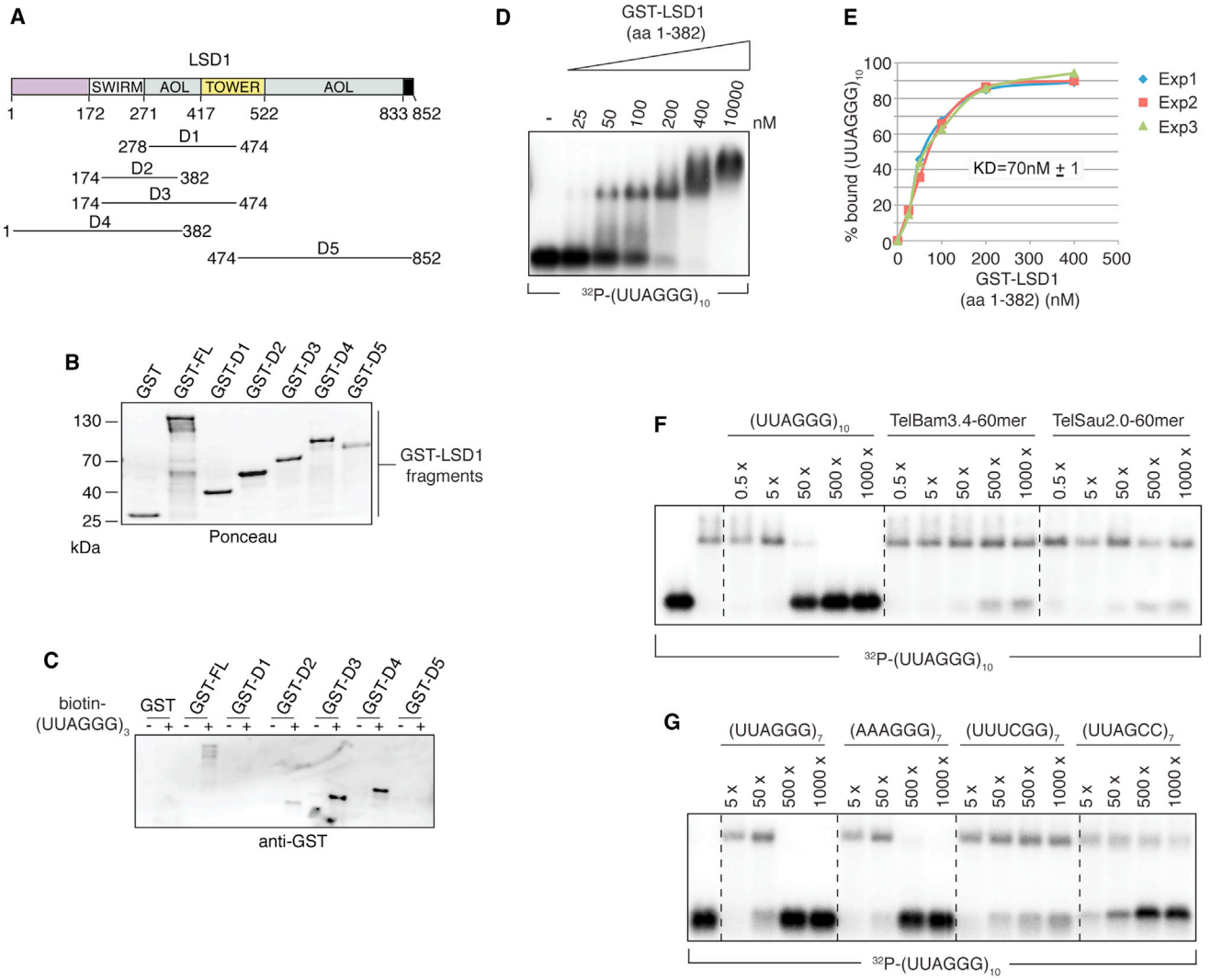

Figure 2. LSD1 Preferentially Binds UUAGGG-TERRA Repeats

(A) Scheme of LSD1 deletion mutants.

(B) Ponceau staining was used to evaluate the expression of LSD1 deletion mutants.

(C) Western blotting was used to evaluate the binding of GST-LSD1 deletion mutants to NeutrAvidin bead-bound biotinylated $(UUAGGG)_3$ oligonucleotide.

(D) Agarose EMSA was used to measure LSD1 RNA binding activity in vitro. GST-LSD1 fragment D4 (aa 1–382) was assayed for binding to ^{32}P-$(UUAGGG)_{10}$ RNA oligonucleotide.

(E) K_D measurement of GST-LSD1 fragment D4 (aa 1–382) binding to ^{32}P-$(UUAGGG)_{10}$ RNA oligonucleotide. Exp1, experiment 1; Exp2, experiment 2; Exp3, experiment 3.

(F) EMSA competition experiment with GST-LSD1 fragment D4 (aa 1–382) binding to ^{32}P-$(UUAGGG)_{10}$. The fold molar excess of added unlabeled $(UUAGGG)_{10}$, TelBam3.4-60-mer, and TelSau2.0-60-mer competitors is indicated at the top.

(G) EMSA competition experiment of GST-LSD1 fragment D4 (aa 1–382) binding to ^{32}P-$(UUAGGG)_7$ using $(UUAGGG)_7$, $(AAAGGG)_7$, $(UUUCGG)_7$, and $(UUAGCC)_7$ as competitors. Numbers indicate fold excess of competitor over ^{32}P-labeled probe.

See also Figure S2.

depletion (Figures 3A and 3B), suggesting that higher levels of TERRA may enrich LSD1 at damaged chromosome ends. Since RNAi-mediated TERRA downregulation cannot be employed in our study because RNA oligonucleotides of telomeric sequence may perturb telomere integrity by soaking up telomere-associated proteins, we sought to corroborate the link between TERRA levels and LSD1 binding to chromosome ends in human colorectal carcinoma HCT116 cells double knocked out (DKO) for the DNA methyltransferases *DNMT1* and *DNMT3b* (Rhee et al., 2002), in which TERRA is highly expressed and remains associated with telomeric chromatin (Farnung et al., 2012). We infected the parental (par) and the DKO cells with retroviruses expressing a dominant-negative mutant of TRF2, $TRF2^{\Delta B \Delta M}$, that strips TRF2 and its interacting factors off the telomeres (van Steensel et al., 1998; Zhu et al., 2000) and causes DDR activation, loss of telomeric G overhangs, chromosome fusions, and genome

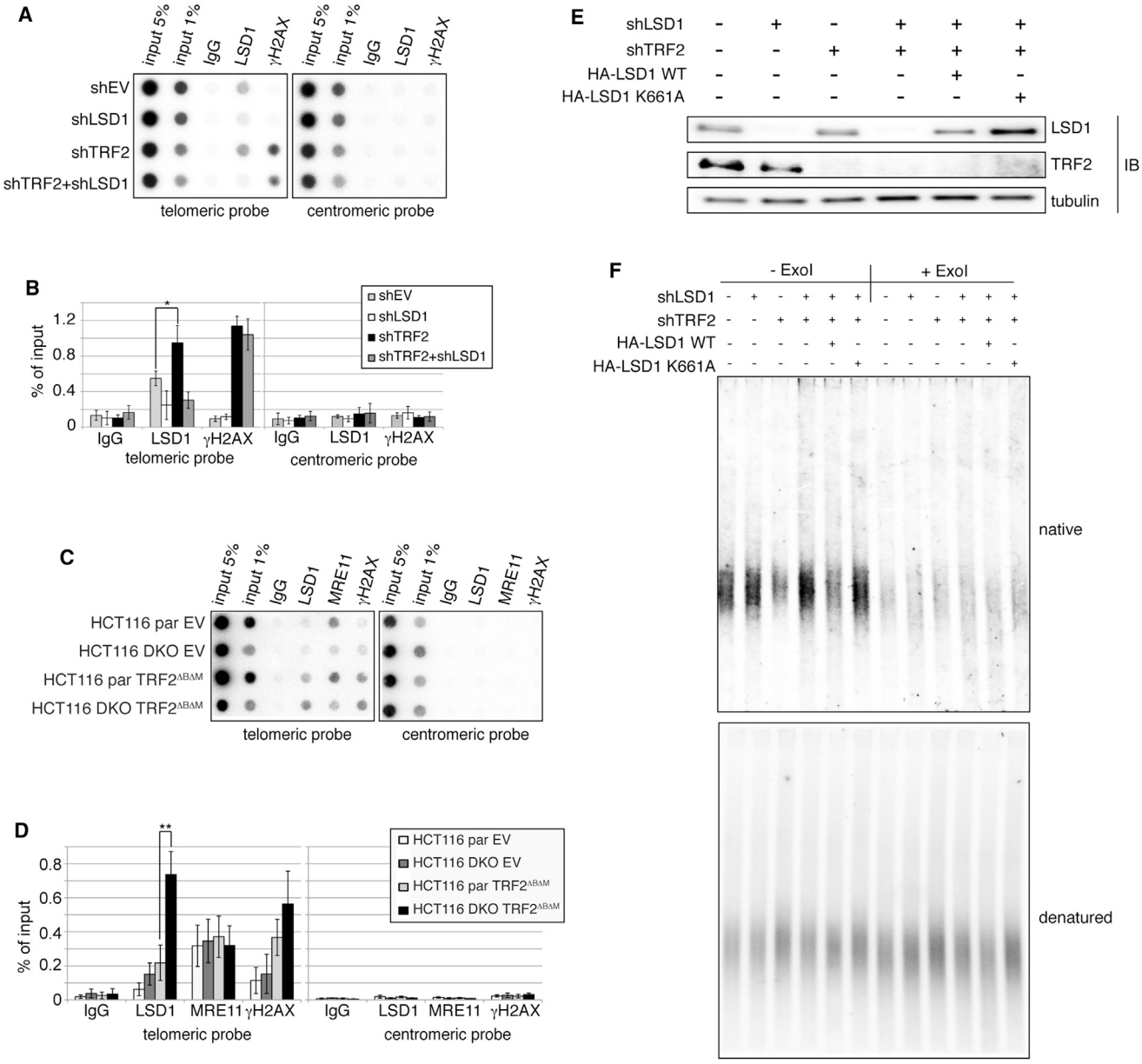

Figure 3. LSD1 Is Recruited to Uncapped Telomeres and Is Required for 3′ G Overhang Removal

(A) ChIP of telomeric and centromeric DNA with LSD1 and γH2AX antibodies was performed in HeLa cells transfected with control vector (shEV) or depleted for LSD1 (shLSD1), TRF2 (shTRF2), or both (shTRF2+shLSD1).

(B) Quantification of three different ChIP experiments represented by (A) (mean ± SD, n = 3). Statistical analysis was done using a two-tailed Student's t test (*$p < 0.05$).

(C) ChIP of telomeric and centromeric DNA with LSD1 and γH2AX antibodies was performed in HCT116 par and *DNMT1* and *DNMT3b* DKO cells infected with retroviruses expressing dominant-negative TRF2$^{\Delta B\Delta M}$ or empty vector.

(D) Quantification of three different ChIP experiments represented by (C) (mean ± SD, n = 3). Statistical analysis was done using a two-tailed Student's t test (**$p < 0.01$).

(E) Western blot analysis of HeLa cell extracts expressing shRNA constructs and shRNA-resistant forms of LSD1 WT and LSD1 K661A.

(F) TRF analysis was used to detect the telomeric 3′ G overhang from HeLa cells transfected with the indicated plasmids. A radiolabeled telomeric probe was annealed to native DNA detecting the single-strand (ss) telomeric signal (upper panel). ExoI (+ExoI) treatment removes the terminal telomeric 3′ G overhang. The total telomeric DNA is detected upon denaturation of the DNA (lower panel).

See also Figures S3 and S4.

instability (de Lange, 2004; Karlseder et al., 1999, 2002; Smogorzewska et al., 2002; Stansel et al., 2001; van Steensel et al., 1998). Compared to the par cells, which have longer telomeres and low TERRA levels, DKO cells showed strongly enhanced LSD1 recruitment upon expression of dominant-negative TRF2$^{\Delta B\Delta M}$ (Figures 3C and 3D), thus supporting the notion that TERRA may promote LSD1 binding to dysfunctional telomeres. However, indirect effects due to the absence of the DNA methyltransferases could not be excluded. For all these experiments, the DNA-damage marker γ-H2AX was monitored and served as a control to evaluate the functional efficiency of TRF2 inactivation (Figures 3A–3D). Taken together, these data suggest that LSD1 binds to chromosome termini and that TERRA upregulation may enhance LSD1 recruitment in the context of dysfunctional telomeres.

LSD1 Does Not Affect Telomeric Chromatin but Is Required for the Processing of Uncapped Chromosome Ends

LSD1 is known to demethylate the mono- and dimethyl forms of lysine 4 (H3K4) (Shi et al., 2004) and 9 (H3K9) (Metzger et al., 2005) of histone 3. Because LSD1 strongly associates with dysfunctional telomeres, we investigated by ChIP a putative role for LSD1 in controlling the histone methylation pattern upon telomere uncapping (Figures S3A and S3B). The density of mono- and dimethylated H3K4 across telomeres was not affected following TRF2 depletion. On the contrary, dimethylated H3K9 (H3K9 me2) and, to a much lesser extent, monomethylated H3K9 (H3K9 me1) were decreased at chromosome ends upon telomere uncapping, whereas they remained unaltered at centromeric chromatin. However, the changes in the histone methylation pattern at damaged telomeres appear not to rely on LSD1 because the reduced density of mono- and dimethylated H3K9 at dysfunctional telomeres was not rescued by the concomitant depletion of TRF2 and LSD1 (Figures S3A and S3B). Recently, it has been shown that LSD1 also controls the methylation status of nonhistone proteins (Cho et al., 2011; Huang et al., 2007; Kontaki and Talianidis, 2010; Wang et al., 2009). To define a putative nonhistone LSD1 target at telomeres, we examined whether telomeric phenotypes elicited upon removal of TRF2 can be reversed by LSD1 depletion. Damaged telomeres accumulate TIFs (Takai et al., 2003; Zhu et al., 2003). TIF formation can be detected via the association of the DNA-damage proteins γH2AX and 53BP1 with telomeres. In immunofluorescence (IF)-fluorescence in situ hybridization (FISH) experiments, we found that the DNA-damage marker 53BP1 accumulated with a similar frequency at telomeres of TRF2-depleted and TRF2/LSD1 double-depleted cells (Figures S3C and S3D). This indicates that TIF formation is not affected by LSD1 in TRF2-deficient cells.

TRF2 removal leads to a rapid loss of the telomeric 3′ G overhang signal and telomere fusions by NHEJ (Celli and de Lange, 2005; Zhu et al., 2003). Assessment of telomeric G overhang by native in-gel hybridization revealed that the 3′ G overhang signal was reduced in TRF2-deficient cells as expected but that it persisted upon concomitant depletion of TRF2 and LSD1 (Figures 3E and 3F). Furthermore, expression of the shRNA-resistant LSD1 WT, but not the demethylase-impaired mutant K661A (Lee et al., 2005) (Figure S4A), restored 3′ G overhang processing in TRF2-depleted cells (Figures 3E and 3F). Treatment with the 3′ end-specific bacterial ExoI confirmed that the detected single-stranded telomeric DNA was terminal. These results were confirmed by analyzing the same DNA samples in parallel (Figures S4B and S4C) by native in-gel hybridization and an independent assay involving a duplex-specific nuclease (DSN), which digests double-stranded genomic DNA and leaves the single-stranded overhangs intact (Zhao et al., 2011). The telomere single-strand G-rich overhang was detected by Southern hybridization (Figure S4B). Also in this assay, depletion of TRF2 reduced the G overhang signal, whereas the signal was retained in TRF2 and LSD1 double-depleted cells. Double depletion of TRF2 and MRE11 (Figure S4D) also did not lead to loss of the 3′ G overhang, consistent with the fact that MRE11 is required for 3′ G overhang removal (Figure S4E). The LSD1 knockdown did not affect cell-cycle progression (Figures S4F and S4G), ruling out the possibility that the observed phenotype was due to alterations of the cell-cycle profile. Despite the fact that removal of the 3′ G overhang is a prerequisite for NHEJ at chromosome ends (Zhu et al., 2003), the frequency of telomere fusions observed in metaphase spreads upon TRF2 depletion was not affected by LSD1 knockdown (Figures S4H and S4I). This suggests that LSD1 depletion may have slowed down but not prevented overhang removal. Overall, these data indicate that LSD1, through its demethylase activity, promotes G overhang resection at uncapped telomeres.

LSD1 Interacts with MRE11

We further reasoned that LSD1 may activate the MRE11 or ERCC1/XPF nuclease to remove telomeric 3′ G overhangs from uncapped telomeres (Attwooll et al., 2009; Deng et al., 2009a; Zhu et al., 2003). We tested for a physical interaction between LSD1 and MRE11 by reciprocal coimmunoprecipitation (Figures 4A and 4B). Proteins in HeLa cell nuclear extracts were immunoprecipitated with antibodies against endogenous LSD1, MRE11, or IgG, which served as negative control. We observed that LSD1 specifically coimmunoprecipitated MRE11 and vice versa, indicating that the two proteins can reside in the same complex (Figure 4A). No interaction was found between endogenous LSD1 and XPF nor LSD1 and other proteins involved in 3′ G overhang processing or in the activation of the telomeric DDR (Figure S5). Notably, telomere uncapping by depletion of TRF2 increased the interaction between LSD1 and MRE11 (Figure 4A). Furthermore, we found that also ectopically expressed HA-tagged LSD1 and myc-tagged MRE11 associated in HEK293T cells (Figure 4B). We next sought to identify the MRE11 domain responsible for the interaction with LSD1. We generated different GST-MRE11 deletion mutants (Figure 4C) and purified them from recombinant *E. coli*. We then incubated glutathione agarose beads-immobilized GST-MRE11 fragments with purified recombinant HA-tagged LSD1 in vitro. We found that HA-LSD1 interacted with a C-terminal region of MRE11 encompassing the GAR motif and amino acids adjacent to the DNA binding domain (Figure 4D). On the other side, we performed an analogous experiment to determine which domain of LSD1 is involved in the interaction with MRE11. Purified GST-LSD1 fragments were incubated with purified 3×FLAG-MRE11. We observed

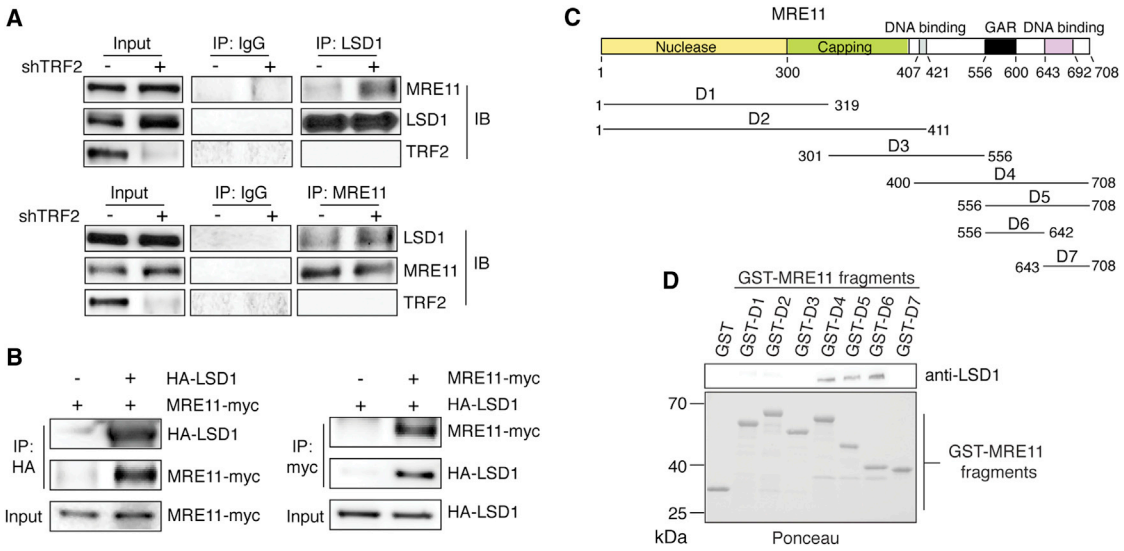

Figure 4. LSD1 Directly Interacts with MRE11

(A) Reciprocal coimmunoprecipitation assay was used to detect the interaction between endogenous LSD1 and MRE11 in HeLa transfected with control vector (shEV) or depleted for TRF2 (shTRF2).

(B) Reciprocal coimmunoprecipitation assay was used to detect the interaction between ectopic HA-LSD1 and MRE11-myc in HEK293T cells.

(C) Scheme of MRE11 deletion mutants.

(D) Purified HA-LSD1 was incubated with the indicated glutathione bead-bound GST-MRE11 fragments. Western blotting was used to evaluate which GST-MRE11fragment is able to retain HA-LSD1 in vitro.

See also Figure S5.

that the SWIRM/AOL-N-ter domain of LSD1, responsible for the interaction with TERRA (Figures 2A–2C), is also required for the binding to MRE11 (Figures 5A and 5B). Thus, TERRA and MRE11 associate with the same domain of LSD1 (Figure 5C).

TERRA Reinforces the Interaction between LSD1 and MRE11

Next, we explored whether TERRA regulates the strength of LSD1-MRE11 interaction. We carried out biochemical experiments in which bead-bound GST-LSD1 was incubated with 3× FLAG-MRE11 in the presence of increasing amounts of $(UUAGGG)_{10}$ RNA oligonucleotide. TERRA-mimicking oligonucleotide increased the amount of 3×FLAG-MRE11 captured by GST-LSD1 up to 9-fold (Figure 5D), whereas control oligonucleotide did not influence the binding (Figure S6A). Similarly, association of LSD1 and MRE11 was enhanced in HEK293T cells transfected with $(UUAGGG)_{10}$ TERRA but not with control RNA oligonucleotides (Figure S6B). However, only LSD1 but not MRE11 (data not shown) binds TERRA in a detectable manner, suggesting that TERRA does not bridge their interaction.

LSD1 Associates with Dysfunctional Telomeres in an MRN-Dependent Manner

Because MRE11 plays a critical role in sensing dysfunctional telomeres by promoting the activation of ATM-dependent DNA-damage signaling pathways, we further examined whether the LSD1 binding to deprotected telomeres can be affected by the MRN complex. For this purpose, we performed ChIP experiments in TRF2-deficient cells depleted for MRE11 or NBS1 (Figure S6C), and we found that LSD1 no longer accumulated efficiently at damaged chromosome ends (Figures 5E and 5F). Therefore, the MRN complex is critical for LSD1 retention at dysfunctional telomeres. On the other hand, LSD1 did neither affect the binding of MRE11 to telomeres (Figures S6D–S6F) nor the formation of the MRN complex (Figure S6G).

LSD1 Stimulates MRE11 Nuclease Activities In Vitro

MRE11 exhibits exonuclease activity on DNA double-stranded blunt end and 3′-recessed substrates as well as endonuclease activity on hairpin substrates (Paull and Gellert, 1998). In order to test for effects of LSD1 on MRE11 nuclease activity, we carried out in vitro assays (Lee et al., 2003). We purified WT and the presumed nuclease-deficient $MRE11^{H129N}$ mutant (Deng et al., 2009a) from human HEK293T cells (Figure 6A) and measured exo- and endonuclease activities. MRE11 WT but not the H129N mutant exhibited exo- and endonuclease activity as expected (Figures 6B and 6C). In order to evaluate a contribution of LSD1, we expressed 3×FLAG-tagged MRE11 in HEK293T cells alone or in combination with HA-LSD1 WT or HA-LSD1 K661A demethylation-impaired mutant (Lee et al., 2005) (Figure 6D). When 3×FLAG-MRE11 was purified from HA-LSD1 WT-expressing cells, MRE11 showed an enhanced exonuclease activity if compared to the MRE11 purified from WT cells or from cells expressing catalytically impaired HA-LSD1 K661A (Figure 6E). A similar result was obtained when 3×FLAG-MRE11 and HA-LSD1 were purified separately and coincubated in the nuclease assays (Figure S7A). Incubation of 3×FLAG-MRE11 with HA-LSD1 but not with BSA stimulated the MRE11 exonuclease activity (Figure S7B). Addition of a specific LSD1 inhibitor (Inhibitor IV; Calbiochem) reduced the LSD1-mediated

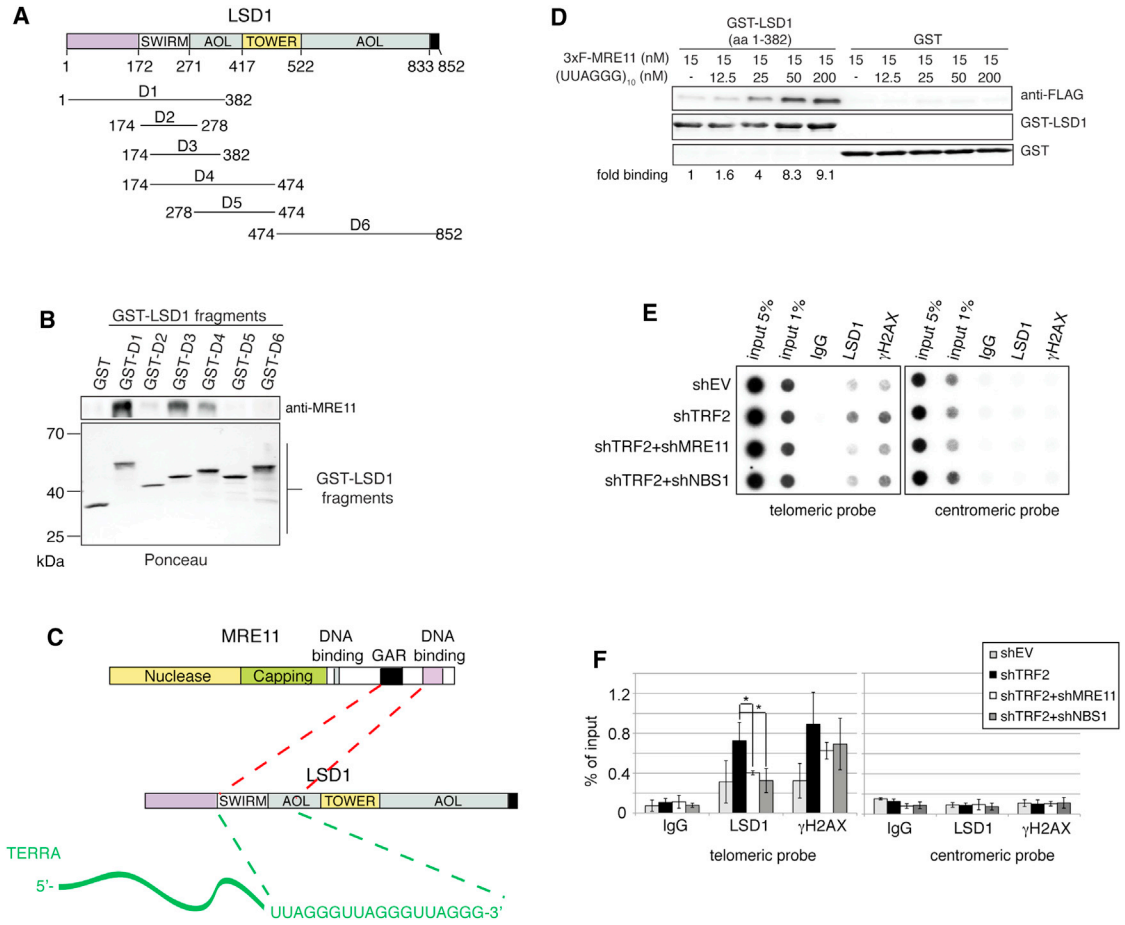

Figure 5. MRE11 Interacts with the SWIRM/AOL-N-ter Domain of LSD1, and TERRA Stabilizes the Interaction between the Two Proteins

(A) Scheme of LSD1 deletion mutants.

(B) Western blotting was used to evaluate the binding of GST-LSD1 deletion mutants to purified 3×FLAG-MRE11.

(C) Scheme of the interaction domains required for the association of LSD1 with TERRA and MRE11.

(D) Binding of affinity-purified 3×FLAG-MRE11 to glutathione bead-bound GST-LSD1 fragment D4 (aa 1–382) or GST in the presence of increasing amounts of $(UUAGGG)_{10}$.

(E) ChIP of telomeric and centromeric DNA with LSD1 and γH2AX antibodies was performed in HeLa cells transfected with control vector (shEV) or depleted for TRF2 (shTRF2), TRF2, and MRE11 (shTRF2+shMRE11) and TRF2 and NBS1 (shTRF2+shNBS1).

(F) Quantification of three different ChIP experiments represented by (E) (mean ± SD, n = 3). Statistical analysis was done using a two-tailed Student's t test (*$p < 0.05$).

F, FLAG. See also Figure S6.

stimulation of MRE11 (Figure S7C). Furthermore, LSD1 WT and, to a lesser extent, LSD1 K661A enhanced also the MRE11 endonuclease activity (Figure 6F). Altogether, these findings demonstrate that LSD1 stimulates the exo- and endonuclease activities of MRE11.

DISCUSSION

In this study, we identify TERRA and LSD1 as actors at deprotected telomeres that follow TRF2 depletion, and we provide evidence that TERRA and LSD1 collaborate with MRE11 in the processing of the 3′ G overhangs. Our results demonstrate that MRE11 as part of the MRN complex is required for LSD1 stabilization at uncapped telomeres. We demonstrate that LSD1 directly interacts with MRE11 and that the SWIRM/AOL-N-ter domain of LSD1 mediates the binding to the C-terminal region of MRE11 encompassing the GAR motif. We also provide evidence that TERRA promotes the interaction between LSD1 and MRE11. First, increased TERRA levels upon TRF2 depletion correlate with enhanced LSD1 recruitment at dysfunctional telomeres in HeLa cells. Second, enhanced TERRA levels in HCT116 DKO versus HCT116 WT cells correlate with increased LSD1 recruitment upon telomere uncapping. Third, and most strikingly, TERRA strongly enhances the binding affinity between MRE11 and LSD1 in vitro with purified proteins and in vivo upon transfection of TERRA RNA oligonucleotides. We also find that LSD1 but not MRE11 binds TERRA. Therefore, TERRA seems not to bridge their interaction. However, when associated with

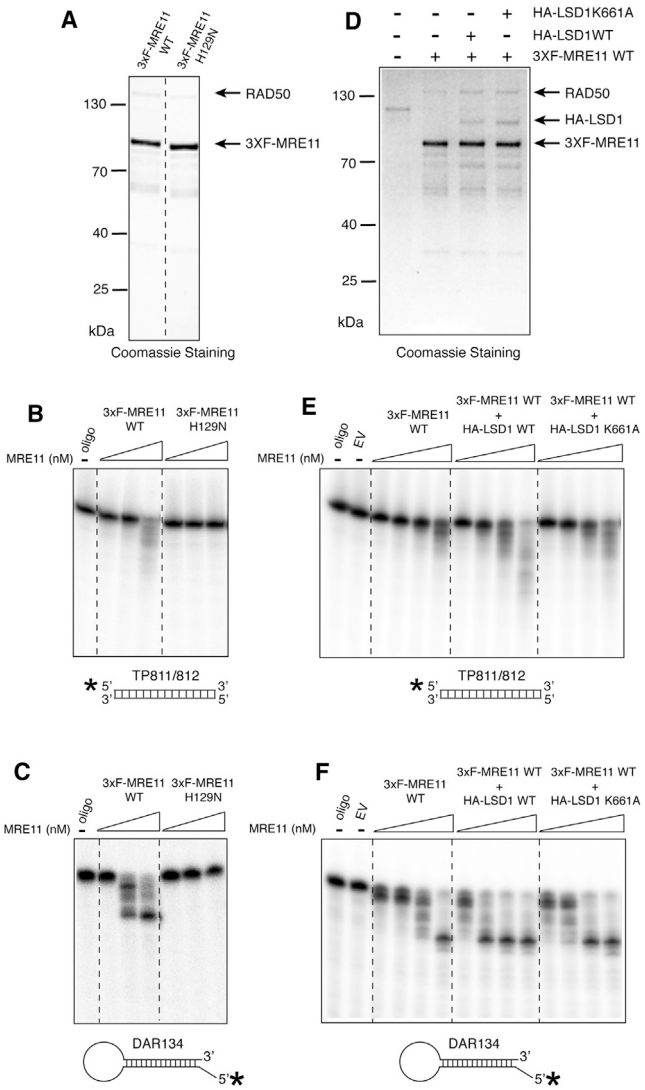

Figure 6. LSD1 Stimulates the MRE11 Exo- and Endonuclease

(A) Coomassie staining was used to detect 3×FLAG-MRE11 WT and H129N affinity purified from HEK293T cells.

(B) Exonuclease assays were performed with increasing concentrations (2, 4, 10, and 20 nM) of 3×FLAG-MRE11 WT or H129N mutant, purified from HEK293T.

(C) Endonuclease assays were performed with increasing concentrations (12.5, 25, 50, and 100 nM) of 3×FLAG-MRE11 WT or H129N mutant, purified from HEK293T.

(D) Coomassie staining was used to detect 3×FLAG-MRE11 WT co-transfected with empty vector, HA-LSD1 WT, or HA-LSD1 K661A plasmids. Immunoprecipitated material from HEK293T cells transfected with empty vector only was used as negative control.

(E) Exonuclease assays were performed with increasing concentrations (2, 4, 10, and 20 nM) of 3×FLAG-MRE11 WT cotransfected or not with HA-LSD1 WT or HA-LSD1 K661A catalytically impaired mutant.

(F) Endonuclease assays were performed with increasing concentrations (12.5, 25, 50, and 100 nM) of 3×FLAG-MRE11 WT cotransfected or not with HA-LSD1 WT or HA-LSD1 K661A catalytically impaired mutant.

See also Figure S7.

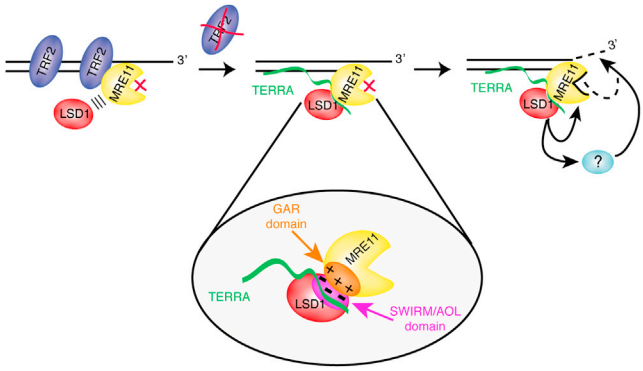

Figure 7. Proposed Model for the Function of TERRA and LSD1 at Uncapped Telomeres

Depletion of TRF2 leads to increased TERRA levels and recruitment of LSD1 to uncapped telomeres. LSD1 recruitment requires MRE11 and may be promoted by TERRA, which enhances the affinity between LSD1 and MRE11. LSD1 stimulates the exo- and endonuclease activities of MRE11. LSD1 recruitment to uncapped telomeres triggers removal of the telomeric 3′ G overhang through MRE11 and possibly other LSD1 substrates.

LSD1, the negatively charged phosphate-sugar backbone of TERRA might attract the abundant arginine residues of the GAR domain in MRE11 (Figure 7). Alternatively, TERRA might have allosteric effects on LSD1 increasing its affinity for MRE11.

TERRA directly interacts with the SWIRM/AOL-N-ter domain of LSD1. The SWIRM domain is found in several chromatin-modifying complexes (Nicholson and Chen, 2009) and has been implicated in binding nucleosomal and free double-stranded DNA. However, the SWIRM domain of LSD1 lacks DNA binding activity (Yoneyama et al., 2007), and our results indicate that it contributes to directly bind RNA. Our mutational analyses reveal that perturbation of the AGGG sequence within the UUAGGG repeats strongly reduces the association between TERRA and LSD1, thus suggesting that LSD1 can bind unfolded UUAGGG repeats. However, because the UUAGGG repeats of TERRA can fold into parallel-stranded G quadruplex structures (Martadinata et al., 2011; Martadinata and Phan, 2013; Xu et al., 2010), it is possible that LSD1 instead recognizes TERRA quadruplexes. LSD1 complexes were previously found in association with the long noncoding RNA HOTAIR, but this interaction appeared to be indirect because purified LSD1 lacked HOTAIR binding activity (Tsai et al., 2010). Thus, we report here direct LSD1-RNA interaction.

What are the roles of LSD1 at uncapped telomeres? We find that LSD1 is required for efficient resection of the 3′ G overhang at dysfunctional telomeres because its depletion leads to persistence of the 3′ G overhang in TRF2-depleted cells. Our results also indicate that LSD1 exerts its effects on the 3′ G overhang through MRE11 (Figure 7). Strikingly, LSD1 stimulates the endo- and exonuclease activities of MRE11 when coexpressed with MRE11 in HEK293 cells prior to purification of MRE11 or when added to the in vitro reaction. The lysine demethylation activity of LSD1 appears involved in the stimulation of MRE11 because K661A mutant LSD1 had a reduced ability to activate MRE11 in vitro and telomeric 3′ G overhang removal in vivo.

Similarly, addition of the LSD1 small molecule inhibitor reduced the stimulatory effects of LSD1. This suggests that MRE11 may contain methylated lysine residues that inhibit its activity. Unexpectedly, LSD1 depletion did not affect the frequency of telomere fusions upon TRF2 depletion in our experiments. 3′ G overhang removal must precede telomere end-joining by the NHEJ machinery (Zhu et al., 2003). We therefore suspect that LSD1 depletion does slow down but not completely abolish the resection of 3′ G overhang at uncapped telomeres. In this scenario, not 3′ G overhang removal but other steps in the reaction are rate limiting for the end-joining of uncapped telomeres such as chromosome end apposition, which becomes rate limiting upon loss of 53BP1 (Dimitrova et al., 2008). While this paper was under review, LSD1 was reported to also associate with internal sites of DNA damage, reducing H3K4 dimethylation and slightly affecting the DDR (Mosammaparast et al., 2013). However, DNA end processing was not assessed in this paper, and at telomeres, contrary to chromosome internal damage sites, LSD1 depletion has no notable effects in histone methylation and 53BP1 recruitment.

In summary, our study provides mechanistic clues into how the MRN complex and TERRA synergize for stabilizing the binding of LSD1 at dysfunctional chromosome ends. LSD1 interacts with and activates MRE11 nuclease activities. This step seems crucial because LSD1 is required for the efficient removal of the 3′ telomeric G overhang though additional activities of MRE11, or different substrates of LSD1 might also contribute to end processing of uncapped telomeres (Figure 7). The here-described mechanism modulates the response to local telomeric DNA damage that occurs upon TRF2 loss, but the same mechanisms may apply during cellular senescence, aging, and accidental or pathological telomere dysfunction events.

EXPERIMENTAL PROCEDURES

Plasmids

shRNA vectors were prepared by cloning double-stranded DNA oligonucleotides into pSuper-Puro or pSuper-Blast. The target sequences were as follows: TRF2, 5′-GCGCATGACAATAAGCAGA-3′; LSD1, 5′-GCACCTTATAA CAGTGATA-3′; MRE11, 5′-TGAGAACTCTTGGTTTAAC-3′; and NBS1, 5′-AG GAAGATGTCAATGTTAG-3′. FL human MRE11 and LSD1-coding sequences were cloned from cDNAs into pCDNA6-based mammalian expression vectors using PCR amplification and In-Fusion cloning (Clontech Laboratories). The FL LSD1 cDNA fragment was subsequently transferred to bacterial expression plasmids pET30a and pGEX6p-1 for His-tagged and GST-tagged LSD1 FL production. pGEX6p1-LSD1 K661A and pCDNA6-HA-LSD1 K661A were obtained using the QuikChange Site-Directed Mutagenesis Kit (Stratagene). MRE11 and LSD1 fragments were cloned into pGEX6p1 bacterial expression vector using PCR amplification and In-Fusion cloning.

Cell Culture and Transfection

HeLa cells were transfected using Lipofectamine 2000 according to the manufacturer's protocol (Invitrogen). Puromycin (2 μg/ml; InvivoGen) or blasticidin (10 μg/ml; InvivoGen) was added to the medium 24 hr after transfection of pSuper-Puro constructs. Puromycin and blasticidin selection was maintained for 4 days.

RNA-IP

RNA-IP assays were performed as described previously by Deng et al. (2009b). More detailed procedures are described in Supplemental Experimental Procedures.

Chromatin Immunoprecipitation

ChIP assays were performed as described previously by Abreu et al. (2010). More detailed procedures are described in Supplemental Experimental Procedures.

EMSA

EMSA for 3×FLAG-MRE11 was performed as described before by Lee et al. (2003). EMSA for GST-LSD1 (aa 1–382) was performed with the following modifications. 1× EMSA reaction buffer for GST-LSD1 (aa 1–382) was composed of 25 mM Tris-HCl (pH 8.0), 100 mM NaCl, 10% glycerol, 2 mM $MgCl_2$, 1 mM DTT, and 1 U/μl SUPERase-IN. A total of 1 nM of ^{32}P-γATP 5′ end-labeled RNA or DNA oligonucleotide probes was mixed with the indicated proteins and competitor oligonucleotides and incubated to equilibrium for 30 min at 37°C. The reaction was supplemented with EMSA loading buffer to a final concentration of 1× (8% glycerol, 2 mM Tris-HCl [pH 7.5], 0.02% bromophenol blue, and cyan cyanol) and separated on 2% 0.5× TBE agarose gels at 60 mA for 30 min. Gels were dried, exposed to Phosphorimager screens, and analyzed using a FLA-3000 Phosphorimager (Fujifilm) and AIDA Image Analyzer software (Raytest).

TRF Analysis and G Overhang Analysis

Following phenol extraction and ethanol precipitation, genomic DNA was digested with RsaI and HinfI and resolved by pulse-field gel electrophoresis on 1% agarose in 0.5× TBE at 5 V cm^{-1} for 16 hr at 14°C with switch times ramped from 0.5 to 6 s. For G overhang analysis, the gel was dried (50°C) and hybridized under native conditions (50°C) for detection of ss telomeric DNA, before denaturation and a second hybridization for total telomeric DNA. For washes, gels were rinsed in 4× SSC and incubated for 30 min at room temperature, followed by successive 30 min washes at 50°C in 4× SSC/0.5% SDS and 2× SSC/0.5% SDS. The ^{32}P-labeled telomeric DNA probe was generated as follows: a template mixture of 1- to 5-kb-long telomeric DNA fragments was synthesized by ligating double-stranded telomeric DNA oligonucleotides $((TTAGGG)_5$, $(CCCTAA)_5)$ that were amplified by PCR. The probe was random labeled with α-^{32}P-dCTP and cold dTTP and dATP (for detection of the TTAGGG strand).

DSN Assay and G Overhang Analysis

Determination of the telomeric G overhang with the DSN method was done as described previously by Zhao et al. (2011).

Protein Purification

HA-, 3×FLAG-, GST-, or His-tagged constructs were purified using anti-HA, M2, and GSH agarose (Sigma-Aldrich) or Ni-NTA agarose (QIAGEN). *E. coli* strain Rosetta (DE3)pLysS (Novagen) was used for all protein expressions in bacteria. Recombinant His-LSD1 was purified using Ni-NTA agarose and imidazole competitor elution. GST-LSD1 FL and fragments as well as GST-MRE11 fragments were purified using GSH agarose and, if needed, eluted using reduced glutathione. HA-LSD1 and 3×FLAG-MRE11 were expressed in HEK293T cells and purified using HA agarose (Sigma-Aldrich) or M2 agarose followed by corresponding competitor peptide elution.

In Vitro MRE11 Nuclease Assays

MRE11 nuclease assays were performed as described by Lee et al. (2003) and Park et al. (2011). Briefly, purified 3×FLAG-MRE11 was preincubated with or without purified HA-LSD1 or BSA and indicated inhibitors for 90 min at 37°C in nuclease reaction buffer (25 mM MOPS [pH 7], 100 mM NaCl, 1 mM $MnCl_2$, and 1 mM DTT), followed by addition of 1 nM of ^{32}P end-labeled nuclease substrate and further incubation overnight at 37°C. Reaction products were analyzed on 15% denaturing polyacrylamide gels, fixed, exposed, and signals revealed using the FLA-3000 Phosphorimager. The LSD1 inhibitor was LSD1 inhibitor IV, RN-1,HCl from Calbiochem. The MRE11 inhibitor was mirin from Sigma-Aldrich.

Antibodies

The following antibodies were used: 53BP1 (NB100-304; Novus Biologicals); Co-REST (07-455; Millipore); Histone H3 (ab1791; Abcam); H3K4me1 (07-436; Millipore); H3K4me2 (07-030; Millipore); H3K9me1 (ab9045; Abcam);

H3K9me2 (ab1220; Abcam); hnRNP A1 (4B10, sc-32301; Santa Cruz Biotechnology); hnRNP K (ab39975; Abcam); LSD1 (ab17721; Abcam); MRE11 (NB100-142; Novus Biologicals); NBS1 (NB100-143; Novus Biologicals); phospho-H2AX (05-636; Millipore); and Rad50 (ab89; Abcam).

Microscopy

TIF analysis by IF-FISH staining was performed as described before (Celli and de Lange 2005). FISH on metaphase spreads was performed as described before (Azzalin et al. 2007).

SUPPLEMENTAL INFORMATION

Supplemental Information includes Supplemental Experimental Procedures and seven figures and can be found with this article online at http://dx.doi.org/10.1016/j.celrep.2014.01.022.

AUTHOR CONTRIBUTIONS

A.P. and S.F. performed the experiments and analyzed the data. A.P., S.F., and J.L. designed the study and wrote the paper.

ACKNOWLEDGMENTS

We thank P. Reichenbach, S. Redon, and I. Zemp for technical help; V. Pfeiffer for critical reading of the manuscript; B. Vogelstein for HCT116 and HCT116-DKO cells; and L. Chen, L. Grolimund, and C.M. Azzalin for sharing reagents and discussions. A.P. was supported in part by an EMBO postdoctoral fellowship, and S.F. was supported in part by a postdoctoral fellowship from the DFG (FE 1205/1-1). Research in J.L.'s laboratory was supported by the Swiss National Science Foundation, a European Research Council advanced investigator grant (grant agreement number 232812), an Initial Training Network grant (CodeAge) from the European Commission's Seventh Framework Programme (grant agreement number 316354), the Swiss Cancer League, and EPFL.

Received: October 4, 2013
Revised: December 18, 2013
Accepted: January 15, 2014
Published: February 13, 2014

REFERENCES

Abreu, E., Aritonovska, E., Reichenbach, P., Cristofari, G., Culp, B., Terns, R.M., Lingner, J., and Terns, M.P. (2010). TIN2-tethered TPP1 recruits human telomerase to telomeres in vivo. Mol. Cell. Biol. *30*, 2971–2982.

Arnoult, N., Van Beneden, A., and Decottignies, A. (2012). Telomere length regulates TERRA levels through increased trimethylation of telomeric H3K9 and HP1α. Nat. Struct. Mol. Biol. *19*, 948–956.

Attwooll, C.L., Akpinar, M., and Petrini, J.H. (2009). The mre11 complex and the response to dysfunctional telomeres. Mol. Cell. Biol. *29*, 5540–5551.

Azzalin, C.M., Reichenbach, P., Khoriauli, L., Giulotto, E., and Lingner, J. (2007). Telomeric repeat containing RNA and RNA surveillance factors at mammalian chromosome ends. Science *318*, 798–801.

Baird, D.M. (2008). Telomere dynamics in human cells. Biochimie *90*, 116–121.

Baumann, P., and Cech, T.R. (2001). Pot1, the putative telomere end-binding protein in fission yeast and humans. Science *292*, 1171–1175.

Burd, C.G., and Dreyfuss, G. (1994). RNA binding specificity of hnRNP A1: significance of hnRNP A1 high-affinity binding sites in pre-mRNA splicing. EMBO J. *13*, 1197–1204.

Caslini, C., Connelly, J.A., Serna, A., Broccoli, D., and Hess, J.L. (2009). MLL associates with telomeres and regulates telomeric repeat-containing RNA transcription. Mol. Cell. Biol. *29*, 4519–4526.

Celli, G.B., and de Lange, T. (2005). DNA processing is not required for ATM-mediated telomere damage response after TRF2 deletion. Nat. Cell Biol. *7*, 712–718.

Cho, H.S., Suzuki, T., Dohmae, N., Hayami, S., Unoki, M., Yoshimatsu, M., Toyokawa, G., Takawa, M., Chen, T., Kurash, J.K., et al. (2011). Demethylation of RB regulator MYPT1 by histone demethylase LSD1 promotes cell cycle progression in cancer cells. Cancer Res. *71*, 655–660.

Cusanelli, E., Romero, C.A., and Chartrand, P. (2013). Telomeric noncoding RNA TERRA is induced by telomere shortening to nucleate telomerase molecules at short telomeres. Mol. Cell *51*, 780–791.

d'Adda di Fagagna, F., Reaper, P.M., Clay-Farrace, L., Fiegler, H., Carr, P., Von Zglinicki, T., Saretzki, G., Carter, N.P., and Jackson, S.P. (2003). A DNA damage checkpoint response in telomere-initiated senescence. Nature *426*, 194–198.

de Lange, T. (2004). T-loops and the origin of telomeres. Nat. Rev. Mol. Cell Biol. *5*, 323–329.

de Lange, T. (2005). Shelterin: the protein complex that shapes and safeguards human telomeres. Genes Dev. *19*, 2100–2110.

de Lange, T. (2009). How telomeres solve the end-protection problem. Science *326*, 948–952.

Denchi, E.L., and de Lange, T. (2007). Protection of telomeres through independent control of ATM and ATR by TRF2 and POT1. Nature *448*, 1068–1071.

Deng, Y., Chan, S.S., and Chang, S. (2008). Telomere dysfunction and tumour suppression: the senescence connection. Nat. Rev. Cancer *8*, 450–458.

Deng, Y., Guo, X., Ferguson, D.O., and Chang, S. (2009a). Multiple roles for MRE11 at uncapped telomeres. Nature *460*, 914–918.

Deng, Z., Norseen, J., Wiedmer, A., Riethman, H., and Lieberman, P.M. (2009b). TERRA RNA binding to TRF2 facilitates heterochromatin formation and ORC recruitment at telomeres. Mol. Cell *35*, 403–413.

Dimitrova, N., Chen, Y.C., Spector, D.L., and de Lange, T. (2008). 53BP1 promotes non-homologous end joining of telomeres by increasing chromatin mobility. Nature *456*, 524–528.

Doksani, Y., Wu, J.Y., de Lange, T., and Zhuang, X. (2013). Super-resolution fluorescence imaging of telomeres reveals TRF2-dependent T-loop formation. Cell *155*, 345–356.

Farnung, B.O., Brun, C.M., Arora, R., Lorenzi, L.E., and Azzalin, C.M. (2012). Telomerase efficiently elongates highly transcribing telomeres in human cancer cells. PLoS One *7*, e35714.

Feuerhahn, S., Iglesias, N., Panza, A., Porro, A., and Lingner, J. (2010). TERRA biogenesis, turnover and implications for function. FEBS Lett. *584*, 3812–3818.

Flynn, R.L., Centore, R.C., O'Sullivan, R.J., Rai, R., Tse, A., Songyang, Z., Chang, S., Karlseder, J., and Zou, L. (2011). TERRA and hnRNPA1 orchestrate an RPA-to-POT1 switch on telomeric single-stranded DNA. Nature *471*, 532–536.

Griffith, J.D., Comeau, L., Rosenfield, S., Stansel, R.M., Bianchi, A., Moss, H., and de Lange, T. (1999). Mammalian telomeres end in a large duplex loop. Cell *97*, 503–514.

Huang, J., Sengupta, R., Espejo, A.B., Lee, M.G., Dorsey, J.A., Richter, M., Opravil, S., Shiekhattar, R., Bedford, M.T., Jenuwein, T., and Berger, S.L. (2007). p53 is regulated by the lysine demethylase LSD1. Nature *449*, 105–108.

Karlseder, J., Broccoli, D., Dai, Y., Hardy, S., and de Lange, T. (1999). p53- and ATM-dependent apoptosis induced by telomeres lacking TRF2. Science *283*, 1321–1325.

Karlseder, J., Smogorzewska, A., and de Lange, T. (2002). Senescence induced by altered telomere state, not telomere loss. Science *295*, 2446–2449.

Klimek-Tomczak, K., Wyrwicz, L.S., Jain, S., Bomsztyk, K., and Ostrowski, J. (2004). Characterization of hnRNP K protein-RNA interactions. J. Mol. Biol. *342*, 1131–1141.

Kontaki, H., and Talianidis, I. (2010). Lysine methylation regulates E2F1-induced cell death. Mol. Cell *39*, 152–160.

Lan, F., Nottke, A.C., and Shi, Y. (2008). Mechanisms involved in the regulation of histone lysine demethylases. Curr. Opin. Cell Biol. *20*, 316–325.

Lee, J.H., Ghirlando, R., Bhaskara, V., Hoffmeyer, M.R., Gu, J., and Paull, T.T. (2003). Regulation of Mre11/Rad50 by Nbs1: effects on nucleotide-dependent

DNA binding and association with ataxia-telangiectasia-like disorder mutant complexes. J. Biol. Chem. *278*, 45171–45181.

Lee, M.G., Wynder, C., Cooch, N., and Shiekhattar, R. (2005). An essential role for CoREST in nucleosomal histone 3 lysine 4 demethylation. Nature *437*, 432–435.

Martadinata, H., and Phan, A.T. (2013). Structure of human telomeric RNA (TERRA): stacking of two G-quadruplex blocks in K(+) solution. Biochemistry *52*, 2176–2183.

Martadinata, H., Heddi, B., Lim, K.W., and Phan, A.T. (2011). Structure of long human telomeric RNA (TERRA): G-quadruplexes formed by four and eight UUAGGG repeats are stable building blocks. Biochemistry *50*, 6455–6461.

Metzger, E., Wissmann, M., Yin, N., Müller, J.M., Schneider, R., Peters, A.H., Günther, T., Buettner, R., and Schüle, R. (2005). LSD1 demethylates repressive histone marks to promote androgen-receptor-dependent transcription. Nature *437*, 436–439.

Mosammaparast, N., Kim, H., Laurent, B., Zhao, Y., Lim, H.J., Majid, M.C., Dango, S., Luo, Y., Hempel, K., Sowa, M.E., et al. (2013). The histone demethylase LSD1/KDM1A promotes the DNA damage response. J. Cell Biol. *203*, 457–470.

Nergadze, S.G., Farnung, B.O., Wischnewski, H., Khoriauli, L., Vitelli, V., Chawla, R., Giulotto, E., and Azzalin, C.M. (2009). CpG-island promoters drive transcription of human telomeres. RNA *15*, 2186–2194.

Nicholson, T.B., and Chen, T. (2009). LSD1 demethylates histone and non-histone proteins. Epigenetics *4*, 129–132.

Okamoto, K., Bartocci, C., Ouzounov, I., Diedrich, J.K., Yates, J.R., 3rd, and Denchi, E.L. (2013). A two-step mechanism for TRF2-mediated chromosome-end protection. Nature *494*, 502–505.

Park, Y.B., Chae, J., Kim, Y.C., and Cho, Y. (2011). Crystal structure of human Mre11: understanding tumorigenic mutations. Structure *19*, 1591–1602.

Paull, T.T., and Gellert, M. (1998). The 3′ to 5′ exonuclease activity of Mre 11 facilitates repair of DNA double-strand breaks. Mol. Cell *1*, 969–979.

Penny, G.D., Kay, G.F., Sheardown, S.A., Rastan, S., and Brockdorff, N. (1996). Requirement for Xist in X chromosome inactivation. Nature *379*, 131–137.

Pfeiffer, V., and Lingner, J. (2012). TERRA promotes telomere shortening through exonuclease 1-mediated resection of chromosome ends. PLoS Genet. *8*, e1002747.

Porro, A., Feuerhahn, S., Reichenbach, P., and Lingner, J. (2010). Molecular dissection of telomeric repeat-containing RNA biogenesis unveils the presence of distinct and multiple regulatory pathways. Mol. Cell. Biol. *30*, 4808–4817.

Redon, S., Reichenbach, P., and Lingner, J. (2010). The non-coding RNA TERRA is a natural ligand and direct inhibitor of human telomerase. Nucleic Acids Res. *38*, 5797–5806.

Redon, S., Zemp, I., and Lingner, J. (2013). A three-state model for the regulation of telomerase by TERRA and hnRNPA1. Nucleic Acids Res. *41*, 9117–9128.

Rhee, I., Bachman, K.E., Park, B.H., Jair, K.W., Yen, R.W., Schuebel, K.E., Cui, H., Feinberg, A.P., Lengauer, C., Kinzler, K.W., et al. (2002). DNMT1 and DNMT3b cooperate to silence genes in human cancer cells. Nature *416*, 552–556.

Schoeftner, S., and Blasco, M.A. (2008). Developmentally regulated transcription of mammalian telomeres by DNA-dependent RNA polymerase II. Nat. Cell Biol. *10*, 228–236.

Shi, Y., Lan, F., Matson, C., Mulligan, P., Whetstine, J.R., Cole, P.A., Casero, R.A., and Shi, Y. (2004). Histone demethylation mediated by the nuclear amine oxidase homolog LSD1. Cell *119*, 941–953.

Smogorzewska, A., Karlseder, J., Holtgreve-Grez, H., Jauch, A., and de Lange, T. (2002). DNA ligase IV-dependent NHEJ of deprotected mammalian telomeres in G1 and G2. Curr. Biol. *12*, 1635–1644.

Stansel, R.M., de Lange, T., and Griffith, J.D. (2001). T-loop assembly in vitro involves binding of TRF2 near the 3′ telomeric overhang. EMBO J. *20*, 5532–5540.

Takai, H., Smogorzewska, A., and de Lange, T. (2003). DNA damage foci at dysfunctional telomeres. Curr. Biol. *13*, 1549–1556.

Thisted, T., Lyakhov, D.L., and Liebhaber, S.A. (2001). Optimized RNA targets of two closely related triple KH domain proteins, heterogeneous nuclear ribonucleoprotein K and alphaCP-2KL, suggest Distinct modes of RNA recognition. J. Biol. Chem. *276*, 17484–17496.

Tsai, M.C., Manor, O., Wan, Y., Mosammaparast, N., Wang, J.K., Lan, F., Shi, Y., Segal, E., and Chang, H.Y. (2010). Long noncoding RNA as modular scaffold of histone modification complexes. Science *329*, 689–693.

van Steensel, B., Smogorzewska, A., and de Lange, T. (1998). TRF2 protects human telomeres from end-to-end fusions. Cell *92*, 401–413.

Wang, J., Hevi, S., Kurash, J.K., Lei, H., Gay, F., Bajko, J., Su, H., Sun, W., Chang, H., Xu, G., et al. (2009). The lysine demethylase LSD1 (KDM1) is required for maintenance of global DNA methylation. Nat. Genet. *41*, 125–129.

Wutz, A., Rasmussen, T.P., and Jaenisch, R. (2002). Chromosomal silencing and localization are mediated by different domains of Xist RNA. Nat. Genet. *30*, 167–174.

Xu, Y., Suzuki, Y., Ito, K., and Komiyama, M. (2010). Telomeric repeat-containing RNA structure in living cells. Proc. Natl. Acad. Sci. USA *107*, 14579–14584.

Yehezkel, S., Segev, Y., Viegas-Péquignot, E., Skorecki, K., and Selig, S. (2008). Hypomethylation of subtelomeric regions in ICF syndrome is associated with abnormally short telomeres and enhanced transcription from telomeric regions. Hum. Mol. Genet. *17*, 2776–2789.

Yoneyama, M., Tochio, N., Umehara, T., Koshiba, S., Inoue, M., Yabuki, T., Aoki, M., Seki, E., Matsuda, T., Watanabe, S., et al. (2007). Structural and functional differences of SWIRM domain subtypes. J. Mol. Biol. *369*, 222–238.

Zhao, Y., Shay, J.W., and Wright, W.E. (2011). Telomere G-overhang length measurement method 1: the DSN method. Methods Mol. Biol. *735*, 47–54.

Zhu, X.D., Küster, B., Mann, M., Petrini, J.H., and de Lange, T. (2000). Cell-cycle-regulated association of RAD50/MRE11/NBS1 with TRF2 and human telomeres. Nat. Genet. *25*, 347–352.

Zhu, X.D., Niedernhofer, L., Kuster, B., Mann, M., Hoeijmakers, J.H., and de Lange, T. (2003). ERCC1/XPF removes the 3′ overhang from uncapped telomeres and represses formation of telomeric DNA-containing double minute chromosomes. Mol. Cell *12*, 1489–1498.